JIPB Journal of Integrative Plant Biology

Sucrose transporter2 contributes to maize growth, development, and crop yield[FA]

Kristen A. Leach[1], Thu M. Tran[1], Thomas L. Slewinski[2†], Robert B. Meeley[3] and David M. Braun[1*]

1. Division of Biological Sciences, Interdisciplinary Plant Group, Missouri Maize Center, University of Missouri, Columbia MO 65211 USA
2. Department of Biology, Pennsylvania State University, University Park, PA 16802, USA
3. DuPont Pioneer Research & Development, Johnston, Iowa 50131, USA
[†]Current address: Monsanto Inc., 700 Chesterfield Parkway West, Chesterfield, MO 63017, USA
*Correspondence: David M. Braun (braundm@missouri.edu)
doi: 10.1111/jipb.12527

Abstract During daylight, plants produce excess photosynthates, including sucrose, which is temporarily stored in the vacuole. At night, plants remobilize sucrose to sustain metabolism and growth. Based on homology to other sucrose transporter (SUT) proteins, we hypothesized the maize (*Zea mays*) SUCROSE TRANSPORTER2 (ZmSUT2) protein functions as a sucrose/H^+ symporter on the vacuolar membrane to export transiently stored sucrose. To understand the biological role of *ZmSut2*, we examined its spatial and temporal gene expression, determined the protein subcellular localization, and characterized loss-of-function mutations. *ZmSut2* mRNA was ubiquitously expressed and exhibited diurnal cycling in transcript abundance. Expressing a translational fusion of ZmSUT2 fused to a red fluorescent protein in maize mesophyll cell protoplasts revealed that the protein localized to the tonoplast. Under field conditions, *zmsut2* mutant plants grew slower, possessed smaller tassels and ears, and produced fewer kernels when compared to wild-type siblings. *zmsut2* mutants also accumulated two-fold more sucrose, glucose, and fructose as well as starch in source leaves compared to wild type. These findings suggest (i) ZmSUT2 functions to remobilize sucrose out of the vacuole for subsequent use in growing tissues; and (ii) its function provides an important contribution to maize development and agronomic yield.

Edited by: William J. Lucas, University of California, Davis, USA
Received Dec. 30, 2016; **Accepted** Feb. 10, 2017; **Online on** Feb. 16, 2017
FA: Free Access, paid by JIPB

Research Article

Free Access

INTRODUCTION

Upon assimilation in the photosynthetic mesophyll cells, newly fixed carbon is utilized in cellular respiration, metabolism, transiently stored in the vacuole as sucrose or in plastids as starch, or transported to expanding tissues, typically as sucrose, to provide energy for growth and development or for storage (Kaiser and Heber 1984; Bihmidine et al. 2013; Lucas et al. 2013; Ruan 2014). Stored sugars are remobilized to meet the energy needs of the plant when photosynthesis has diminished due to cloud cover or ceased during the night (Smith and Stitt 2007). Understanding sucrose storage, local transport and long-distance movement is key to improving crop yield (Ayre 2011; Braun et al. 2014; Yadav et al. 2015).

Sucrose can move over short distances between cells that are symplasmically connected through plasmodesmata (PD, e.g., from a mesophyll cell to a bundle sheath cell) (Lucas and Lee 2004). However, long-distance transport through veins requires entry of sucrose into the phloem, and depending on the plant species, may follow different pathways (Rennie and Turgeon 2009; Slewinski and Braun 2010a). In symplasmic phloem loaders, e.g., poplar (*Populus* sp.), sucrose moves entirely through PD down a concentration gradient, from highest in the mesophyll cell cytoplasm to lowest in the phloem cells (the companion cell-sieve element (CC/SE) complexes) (Zhang et al. 2014). However, in apoplasmic phloem loading species, e.g., maize (*Zea mays*) and potato (*Solanum tuberosum*), the CC/SE complex is nearly symplasmically isolated from surrounding cells; hence,

sucrose cannot move effectively through PD into the phloem (Evert et al. 1978; Bürkle et al. 1998). Rather, sucrose must be effluxed across the plasma membrane of the bundle sheath or phloem parenchyma cells into the cell wall (apoplasm), likely by SWEET efflux proteins (Baker et al. 2012; Braun 2012; Chen et al. 2012; Eom et al. 2015), prior to being taken up into phloem CC/SE complex by sucrose transporters or carriers (abbreviated SUTs or SUCs) (Aoki et al. 2003; Lalonde et al. 2004; Sauer 2007).

The SUTs are a small gene family whose members function to control the flux of sucrose across cellular membranes. The SUTs are part of the major facilitator super-family containing 12 transmembrane domains, with most characterized family members functioning as proton-coupled sucrose symporters (Boorer et al. 1996; Chandran et al. 2003; Carpaneto et al. 2005; Reinders et al. 2012). The SUT family has been divided into five distinct clades or groups based on phylogenetic analysis (Braun and Slewinski 2009). Groups 1 and 5 consist entirely of monocot SUTs, group 2 contains only eudicot SUTs, and groups 3 and 4 contain both monocot and eudicot SUTs. For the majority of plant species characterized, only a single group 4 family member is present in each genome (Peng et al. 2014). Of the five SUT groups, only groups 1, 2, and 4 have been characterized in depth. For extensive reviews on SUT functions, please see (Aoki et al. 2003; Lalonde et al. 2004; Sauer 2007; Braun and Slewinski 2009; Kühn and Grof 2010; Ainsworth and Bush 2011; Ayre 2011; Reinders et al. 2012).

Members of groups 1 and 2 were among the first *Sut* genes to be characterized, and several family members function in the apoplasmic phloem loading of sucrose (Riesmeier et al. 1992, 1994; Hirose et al. 1997; Bürkle et al. 1998; Aoki et al. 1999; Gottwald et al. 2000; Hackel et al. 2006; Srivastava et al. 2008; Slewinski et al. 2009). However, plants that use symplasmic sucrose phloem loading also contain *Sut* genes, some of which presumably function to retrieve sucrose lost from the phloem during transport (Zhang and Turgeon 2009; Gil et al. 2011; Zhang et al. 2014). Still other SUT proteins, specifically the group 4 family members, function to remobilize sucrose transiently stored in the vacuole (Reinders et al. 2008; Eom et al. 2011; Payyavula et al. 2011; Schneider et al. 2012). Group 4 *Suts* appear to be broadly expressed, including in many of the tissues examined in *Arabidopsis* (*Arabidopsis thaliana*), poplar (*Populus tremula x alba*), potato, and rice (*Oryza sativa*) (Chincinska et al. 2008; Eom et al. 2011; Payyavula et al. 2011; Schneider et al. 2012). Another nearly universal aspect of group 4 SUTs is their subcellular localization to the tonoplast. Comparison of protein sequences of group 4 SUTs showed they contain a predicted tonoplast protein targeting motif (Reinders et al. 2012). This motif is present in AtSUT4, OsSUT2, HvSUT2, SlSUT4, NtSUT4, LjSUT4, and other group 4 SUTs confirmed to localize to the tonoplast (Endler et al. 2006; Reinders et al. 2008; Eom et al. 2011; Okubo-Kurihara et al. 2011; Schneider et al. 2012). However, group 4 *Sut* mutant phenotypes vary among species, from no observable phenotype in *Arabidopsis*, altered leaf-to-stem ratios in poplar, reduced plant height and altered responses to day length in potato, to reduced height, tiller number, and root weight in rice.

The maize genome contains seven *Sut* genes, of which only *ZmSut1* has been characterized in detail. ZmSUT1 is localized to the CC plasma membrane where it transports sucrose from the apoplasm into the CC. Once imported, sucrose can move through PD into the SE for long-distance transport through the phloem sieve tube (Aoki et al. 1999; Slewinski et al. 2009; Baker et al. 2016). Loss of *ZmSut1* function results in leaf chlorosis, sugar and starch hyper-accumulation in the leaves, strongly reduced fertility, and severe stunting (Slewinski et al. 2009; Slewinski et al. 2010). These phenotypes resemble those of plants missing the SUT primarily responsible for phloem loading in eudicots (Riesmeier et al. 1994; Bürkle et al. 1998; Hackel et al. 2006; Srivastava et al. 2008).

Rice contains five *Sut* genes (Aoki et al. 2003), and the loss-of-function of the orthologous group 1 gene, *OsSut1*, has no obvious morphological phenotypes (Ishimaru et al. 2001; Scofield et al. 2002; Hirose et al. 2010; Eom et al. 2012). Additionally, *ossut1* mutant plants have normal chlorophyll levels in leaves, normal sugars and starch content in leaves, and similar rates of photosynthesis as wild-type plants. These data suggest that OsSUT1 is not essential for apoplasmic phloem loading of sucrose in rice leaves (Eom et al. 2012; Braun et al. 2014). In contrast, loss-of-function of the rice group 4 *Sut*, *OsSut2*, has been proposed to result in a phloem-loading-related phenotype. Eom et al. (2011) isolated a T-DNA mutation in *ossut2*, and

determined that the mutant plants had reduced plant height, tiller numbers, seed weight, and root weight. The mutant leaves contained two-fold higher levels of sucrose, glucose, and fructose, but similar levels of starch as wild type. Intriguingly, Eom et al. (2011) determined that the *ossut2* mutant plants had reduced sugar export from leaves, suggesting that OsSUT2 influences sucrose movement in the phloem. These authors also determined that a green fluorescent protein (GFP) translational fusion to OsSUT2 resides on the tonoplast of mesophyll and bundle sheath cells in leaves, and additionally that *OsSut2* is not expressed in the vasculature (Eom et al. 2011). Collectively, these data were interpreted to suggest that OsSUT2 may regulate the flux of sucrose from the vacuole into the cytoplasm of photosynthetic cells, with the sucrose moving symplasmically through PD into the phloem (Eom et al. 2012). Hence, in contrast to the majority of grasses examined, including maize, barley (*Hordeum vulgare*), wheat (*Triticum aestivum*), sugarcane (*Saccharum* sp.), and sorghum (*Sorghum bicolor*), which are proposed to use apoplasmic sucrose phloem loading (Evert et al. 1978; Thompson and Dale 1981; Robinson-Beers and Evert 1991; Evert et al. 1996; Bihmidine et al. 2015), Eom et al. (2012) suggested that rice may utilize a modified symplasmic sucrose phloem loading pathway.

This intriguing proposition prompted us to investigate the function of the related, sole group 4 gene in the maize genome, *ZmSut2*. ZmSUT2 shares 91% amino acid sequence identity with OsSUT2 and 86% with HvSUT2. ZmSUT2 also contains the predicted tonoplast targeting sequence (Reinders et al. 2012). However, given that maize utilizes apoplasmic sucrose phloem loading, the biological function of *ZmSut2* was unclear. To better understand the contribution of *ZmSut2* to plant growth and development, we characterized its expression and function.

A brief note on nomenclature is needed to clarify some confusion in the field. We refer to the maize group 4 *Sut* gene as *ZmSut2* based on its orthology to the first group 4 *Sut* genes identified in grasses (*HvSut2* and *OsSut2*) (Weschke et al. 2000; Aoki et al. 2003; Braun and Slewinski 2009). However, other workers in the field refer to this same maize gene as *ZmSut4*, based on sequence similarity to eudicot group 4 genes, such as *AtSut4* and *StSut4*. In subsequent research, we suggest the gene be named *ZmSut2*.

RESULTS

ZmSut2 expression analysis

To determine in which tissues *ZmSut2* is expressed, we performed reverse transcription-PCR (RT-PCR) on RNA isolated from several different maize tissues, including juvenile leaf 3, mature adult leaf 8, immature leaf 13, and developing tassel, stem, and roots from greenhouse-grown B73 plants. *ZmSut2* was expressed in all tissues examined (Figure 1A). Data available online from the Maize Gene Expression Atlas: RNA-Seq Expression viewer, which includes microarray and RNA-seq data from 79 different tissues/age combinations (maizegdb.org (Stelpflug et al. 2016)) supports this observation, and indicates that *ZmSut2* is expressed throughout the plant.

To assess whether *ZmSut2* mRNA expression varied throughout the day, leaf tissue was collected every 4 h over a 48 h period from fully expanded mature source leaves (leaf 11) and pale yellow-green, immature sink leaves (leaf 17) ensconced within the whorl of field-grown B73 plants. Quantitative RT-PCR (qRT-PCR) revealed that *ZmSut2* mRNA displayed a strong diurnal expression pattern in source leaves with peak expression occurring between 4:30 pm and 8:30 pm (Figure 1B). Weak diurnal cycling of the *ZmSut2* transcript was also detected in RNA isolated from sink leaves with a similar peak time of expression. As a control to examine diurnal cycling, we analyzed the maize *circadian clock associated* (*ZmCCA*) gene (Ko et al. 2016). *ZmCCA* displayed the expected diurnal cycling with peak expression occurring at 8:30 am (Figure 1C), indicating that the peak in *ZmSut2* expression was not due to any RNA quality or quantity artifacts.

ZmSUT2 protein localizes to the vacuolar membrane

The barley, *Arabidopsis*, tomato (*Solanum lycopersicum*), poplar, rice and other group 4 SUTs were shown previously to localize to the vacuolar membrane (Endler et al. 2006; Reinders et al. 2008; Eom et al. 2011; Payyavula et al. 2011; Schneider et al. 2012). Based on sequence analysis, the maize ZmSUT2 protein is similarly predicted to localize to the tonoplast (Reinders et al. 2012). To determine the subcellular localization of ZmSUT2, we transiently expressed it as a translational fusion to a red fluorescent protein (RFP, ZmSUT2-RFP) in maize mesophyll cell protoplasts. Red fluorescent signal was clearly present on

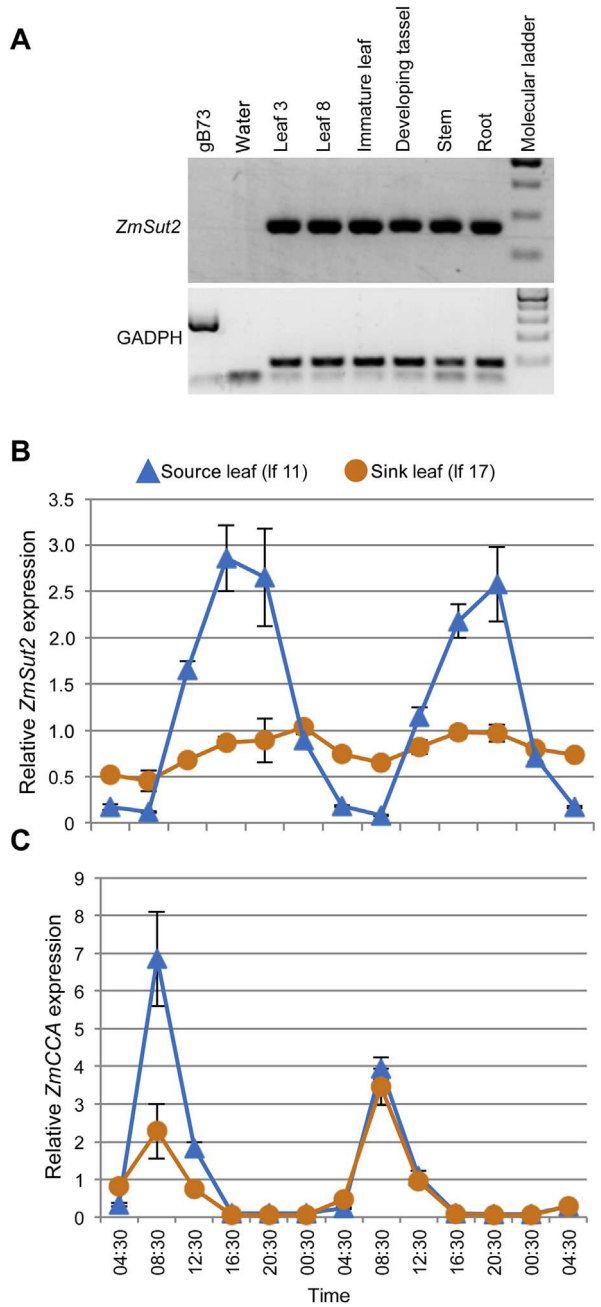

Figure 1. *ZmSut2* mRNA expression analyses
(**A**) RT-PCR examining the expression of *ZmSut2* in greenhouse grown materials. GAPDH expression is shown as a cDNA normalization control. gDNA indicates genomic DNA from the inbred B73 used as a control. Diurnal qRT-PCR analysis of 10 biological replicates per time point from 6-week-old field-grown B73 leaves over a 48 h diurnal cycle for (**B**) *ZmSut2* and (**C**) *ZmCCA* in mature adult leaves and immature leaves. Error bars represent standard error. Blue triangles and orange circles in (**B**) and (**C**) represent source leaf 11 (lf 11) and sink leaf 17 (lf 17), respectively. Dawn was at 5:45 am and dusk was at 8:45 pm.

the tonoplast membrane, as well as in other endomembranes, supporting the predicted localization of ZmSUT2-RFP to the vacuolar membrane (arrowheads in Figure 2A–C) and also potentially to the endoplasmic reticulum (Figure 2B, C). Vacuoles from untransformed control protoplasts exhibited no red fluorescence signal (Figure 2D, E).

Isolation of *zmsut2* mutants

To characterize the biological functions of *ZmSut2*, two independent *Mutator (Mu)* transposable element insertion alleles were isolated. Both alleles contained *Mu* insertions in the protein-coding region of the 5' end of the first exon (Figure 3A). The *Mu* insertion sites in *zmsut2-m1* and *zmsut2-m2* (abbreviated collectively as *zmsut2* mutants) were determined to be 139 and 179 bp, respectively, downstream of the translational start site. To determine the effect of the *Mu* insertions on gene function, we examined the RNA levels of the gene in both mutant and wild-type plants during the time interval (between 4:30 and 8:30 pm) at which *ZmSut2* expression was determined by the qRT-PCR results to peak in mature, wild-type leaves (Figure 1B). RT-PCR using primers located in the 3' portion of the *ZmSut2* gene revealed relatively little to no difference in expression between mutant and wild-type plants for both *zmsut2* alleles (Figure 3B). However, when expression was assayed in the 5' region with gene-specific primers flanking the *Mu* insertions, RNA was detected in wild-type plants but not the mutants (Figure 3C). These results suggested the 3' RT-PCR products detected in the mutants originated from a different transcriptional start site. Transcript initiation from within the terminal inverted repeat (TIR) sequences of *Mu* elements has been previously documented (Raizada et al. 2001; Compaan et al. 2003; Slewinski et al. 2009). To determine if the TIR was the origin of the 3' RT-PCR products observed in mutant leaves, RT-PCR was conducted using an upstream-facing gene-specific primer with an outward-facing primer designed to the TIR of *Mu* elements. Products were amplified for both mutants but not the wild type, suggesting transcription initiated from within the *Mu* element (Figure 3D). The PCR products amplified from the mutants with the *Mu* TIR and gene-specific primer were sequenced to determine the coding potential of these transcripts. If translated, the

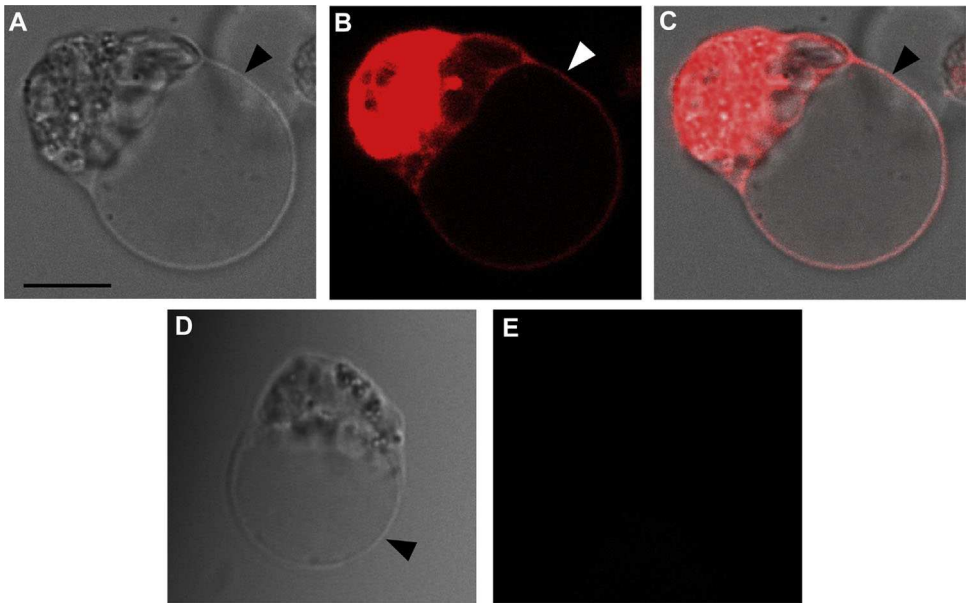

Figure 2. ZmSUT2 is localized to the tonoplast
Confocal microscope images of a vacuole released from a mesophyll cell protoplast transformed with ZmSUT2-RFP (**A**–**C**) and a non-transformed negative control (**D**, **E**). (**A**) Bright-field, (**B**) red fluorescence from ZmSUT2-RFP, and (**C**) panels A and B merged. (**D**) Bright-field, and (**E**) red fluorescence signal in the untransformed control. Arrowheads indicate the tonoplast. Scale bar = 10 μm.

zmsut2-m1 transcript would contain an in-frame stop codon within the transcribed TIR sequence, and would be expected to result in no ZmSUT2 protein being produced. If the *zmsut2-m2* transcript were translated, it would lack the first 59 amino acids, encoding the first and second transmembrane domains. Therefore, these insertion alleles are predicted to be null mutations.

zmsut2 mutants grow slower and have increased sugar content in leaves

To examine the contribution of *ZmSut2* to plant growth, we grew families segregating for *zmsut2-m1* or *zmsut2-m2* in the field. Overall, we observed no profound alterations to plant development or morphology, with the exception that the mutant plants appeared slightly smaller than wild-type siblings. We measured plant height during the growing period to quantify this difference. We found that *zmsut2* mutant plants were significantly shorter at the mid-vegetative stage than wild-type siblings (Figure 4A–D; Table S2).

We postulated that differences in sugar allocation in *zmsut2* mutants versus wild type could account for the plant growth differences. As ZmSUT2 may function to export transitory sucrose stored in the vacuole, we reasoned the mutants would have higher sugar concentrations near dawn, when wild-type sugar levels would be most depleted (Czedik-Eysenberg et al. 2016). To investigate this possibility, mature adult source leaves were harvested from both mutants and their wild-type siblings early in the morning. Sucrose, glucose, fructose, and starch were extracted, and their concentrations determined with High Performance Anion Exchange (HPAE) chromatography. For each sugar analyzed, the mutant contained 34%–146% higher concentrations than wild type (Figure 4E, F). Specifically, in *zmsut2-m1* leaves, the abundance of all three sugars was significantly greater than wild type (Figure 4E). In *zmsut2-m2* leaves, sucrose and glucose contents were significantly higher than in wild type; fructose levels were greater but not significantly different (Figure 4F). Interestingly, no difference was observed in the amount of starch present between mutant and wild-type siblings of both alleles (Figure S1).

To profile these non-structural carbohydrates (NSC) at the end of the day, we quantified sugar and starch accumulation in both mature source

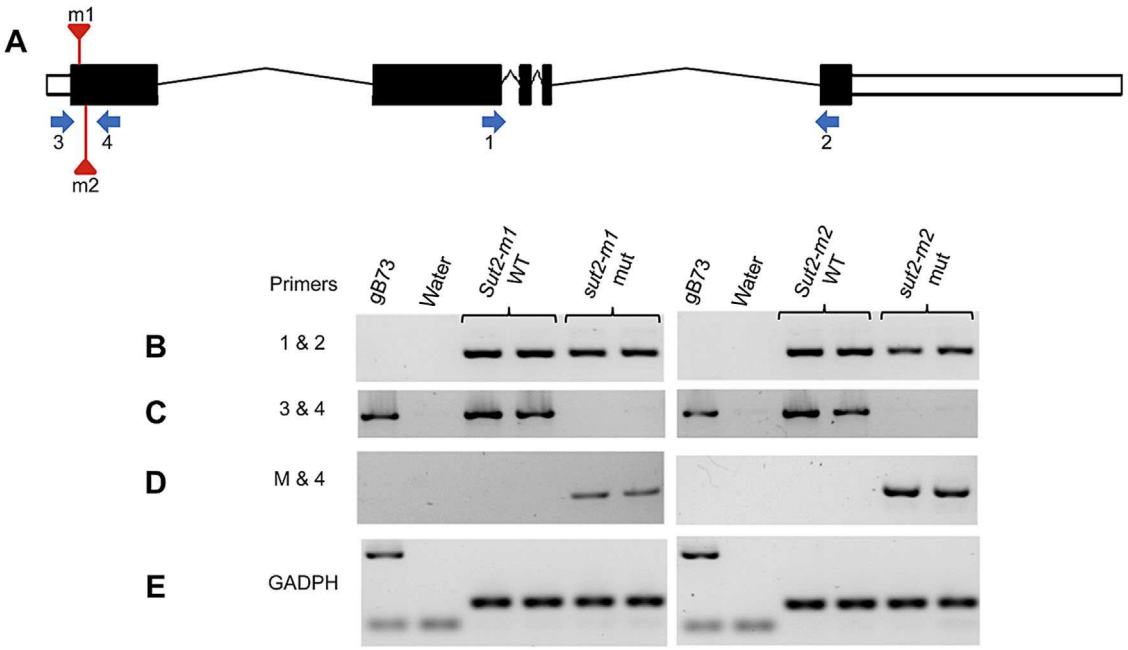

Figure 3. *ZmSut2* map showing location of *Mu* insertions and expression analyses
(**A**) Gene structure and primer locations for *ZmSut2*. Exons are indicated by black boxes, white boxes represent 5' and 3' untranslated regions, and introns are represented by lines. The approximate locations of the *Mu* transposons are located by red triangles located above and below the first exon (m1 and m2). The blue arrows indicate the location of primers utilized for RT-PCR and qRT-PCR (primers 1 and 2), and for genotyping the *zmsut2* mutant (mut) and wild-type (WT) alleles (primers 3 and 4). (**B**–**D**) RT-PCR analysis of transcriptional products from *zmsut2-m1* and *zmsut2-m2*; gB73 is genomic DNA from the inbred B73 (**B**–**E**). (**B**) RT-PCR amplification products produced by primers indicated by arrows 1 and 2. (**C**) Amplification products of primers 3 and 4. (**D**) Amplification products from a primer designed to the terminal inverted repeat of the *Mu* transposon (M) and primer 4. (**E**) GAPDH amplification products shown as a cDNA normalization control.

leaves and immature sink leaves of *zmsut2-m1* and wild-type plants. For the mature source leaves, we observed a significant increase in sucrose, glucose, fructose, and starch (Table 1). Thus, at both time points, the source leaves of *zmsut2* mutants contained approximately a two-fold increase in sucrose and glucose compared with wild-type siblings. Interestingly, in sink leaves, there was no significant difference in the amounts of sucrose and fructose between *zmsut2-m1* mutants and wild type, with the mutant showing slightly more sucrose (~10%) and less fructose (~10%) than wild-type siblings (Table 1). However, a significant difference was observed in the amounts of glucose and starch. Wild-type sink leaves contained 1.2-fold more glucose and 3.3-fold more starch than *zmsut2-m1* mutant sink leaves (Table 1). Overall, these data reveal that *zmsut2* mutant source leaves contained significantly more sugars and starch, whereas the *zmsut2* mutant sink leaves contained either similar or reduced levels of NSC compared to wild-type plants.

Having measured an increase in sugar content in *zmsut2* mutant vs. wild-type source leaves, we measured photosynthetic traits to determine if the NSC accumulation had an effect on photosynthesis and stomatal conductance (Rolland et al. 2006; Slewinski and Braun 2010b; Ruan 2014). Photosynthesis and stomatal conductance were measured twice during plant development, 38 d after planting, and at anthesis. At both time points, no significant difference was observed between *zmsut2-m1* mutant and wild-type plants for these traits (Table 2). A significant difference was observed at 38 days after planting for leaf chlorophyll content, with the *zmsut2-m1* mutant containing approximately 12% less than the wild type; however, no difference in chlorophyll levels was detected at anthesis (Table 2).

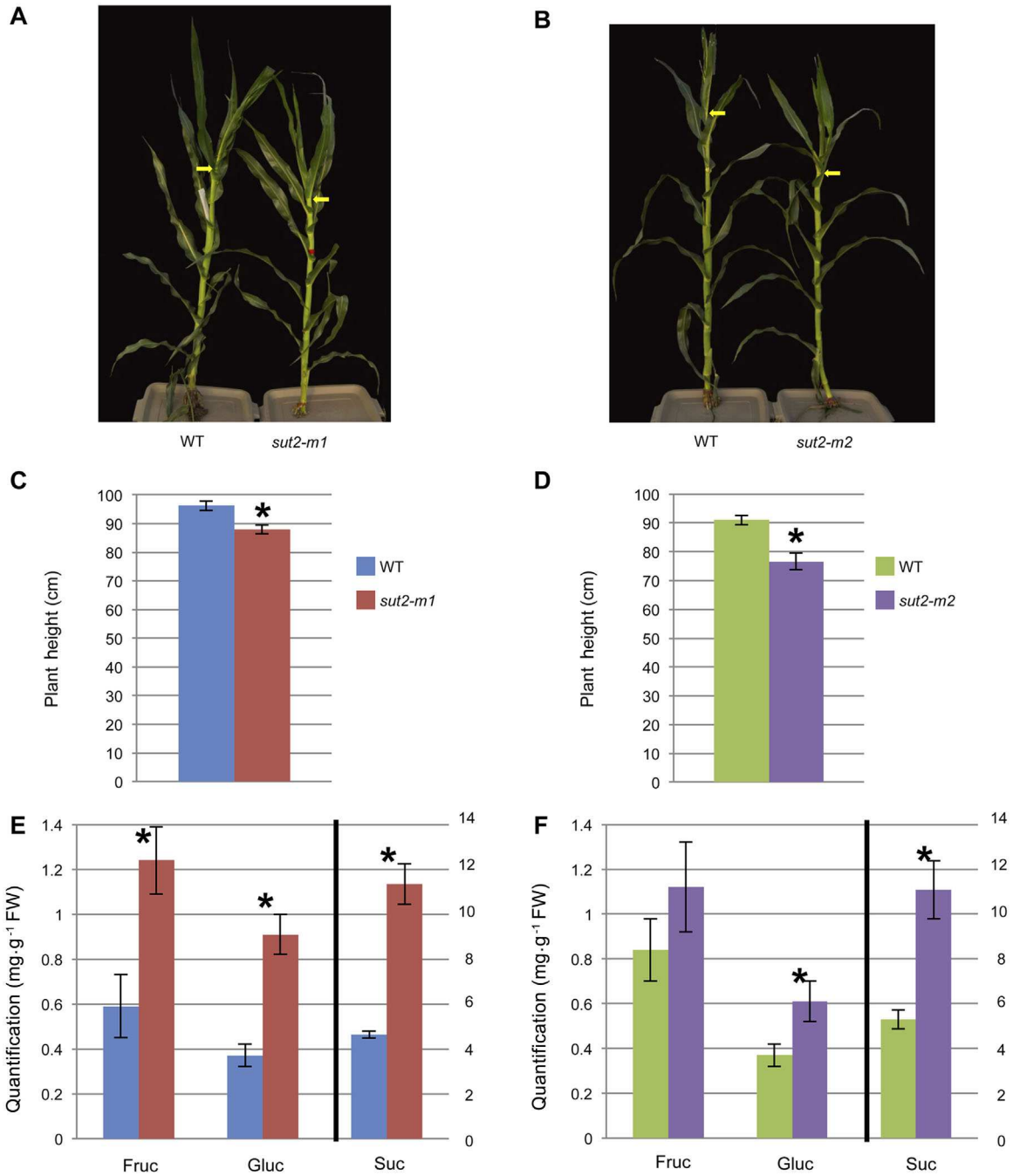

Figure 4. Height and non-structural carbohydrate analysis of field-grown *zmsut2-m1* and *zmsut2-m2* mutant and wild-type (WT) sibling plants

(**A, B**) Photographs of plants representing average plant height. The yellow arrows indicate the position of the ligule of the top most fully expanded leaf from which the height was measured. (**C, D**) Average heights of *zmsut2* mutant and wild-type plants in cm. (**E, F**) Quantification of fructose, glucose, and sucrose in mg · g^{-1} FW at the end of the night in *zmsut2* mutant and wild-type leaves. Error bars represent standard error. An * represents a significant difference at $P \leq 0.05$.

Long-distance sucrose transport in leaves is not altered in *zmsut2* mutants

Previous analyses showed the maize *ZmSut1* gene is essential for sucrose phloem loading (Slewinski et al. 2009; Rotsch et al. 2015; Baker et al. 2016). However, from studies in rice, Eom et al. (2011, 2012) suggested OsSUT2 rather than OsSUT1 functions in sucrose export from leaves. Therefore, we assessed whether

Table 1. Non-structural carbohydrate comparisons between mature source and immature sink leaves of *zmsut2-m1* and wild-type sibling plants at the end of day

Sugar	Geno	*n*	mg · g^{-1} FW	Std Err	*P*-value
Leaf 11 (mature source leaf)					
Suc	WT	6	21.08	1.29	0.0015*
	sut2-m1	6	41	1.5	
Gluc	WT	6	1.05	0.25	0.0018*
	sut2-m1	6	2.58	0.53	
Fruc	WT	6	0.98	0.39	0.0014*
	sut2-m1	6	2.5	0.48	
Starch	WT	6	19.83	1.25	0.0410*
	sut2-m1	5	26.2	0.45	
Leaf 17 (immature sink leaf)					
Suc	WT	6	25.72	0.86	0.3392
	sut2-m1	6	28.57	1.02	
Gluc	WT	6	13.21	0.35	0.0486*
	sut2-m1	5	11.2	0.49	
Fruc	WT	6	4.98	0.5	0.4475
	sut2-m1	6	4.52	0.41	
Starch	WT	5	1.06	0.32	0.0006*
	sut2-m1	6	0.32	0.21	

NSC were quantified (mg · g^{-1} FW) for leaf 11, a mature source leaf, and leaf 17, an immature sink leaf, from *zmsut2-m1* and wild type (WT) leaves. Fruc, fructose; Geno, genotype; Gluc, glucose; *n* = number of biological replicates; Std Err, standard error; Suc, sucrose. *indicates a significant different at $P \leq 0.05$.

ZmSUT2 functions in long-distance sucrose transport in maize leaves. Sucrose movement was analyzed using a radioactive analog of sucrose, 6'-[^{18}F]Fluoro-6'-deoxy-sucrose (Rotsch et al. 2015). Labeled sucrose was applied to the tip of a mature source leaf on intact plants for both *zmsut2* mutants and wild type, followed by translocation for 1 h. The labeled leaves were harvested and exposed to a phosphor imaging plate, and the radioactivity was imaged and quantified (Figures 5, S2). [^{18}F]-labeled sucrose transport appeared indistinguishable between the *zmsut2* mutants and wild type (Figure 5). Quantification of the signal intensity with respect to translocation distance down the leaf blade revealed that similar levels of [^{18}F]-labeled sucrose were transported in *zmsut2* mutants and wild type, with no significant differences detected between the genotypes (Figure S2). In contrast to ZmSUT1, these data suggest ZmSUT2 does not play a predominant role in the apoplasmic transport of sucrose in maize leaves.

Plant competition stress exacerbates aspects of the *zmsut2* mutant phenotype

Because *zmsut2* mutant plants grow more slowly than their wild-type siblings, we hypothesized the mutant phenotype would be increasingly more severe under higher planting densities as the increased plant-plant competition would exacerbate the growth defect associated with NSC retention in mature leaves of *zmsut2* mutant plants. To test this hypothesis, plants segregating 1:1 (mutant:heterozygous) were planted in the field under increasing plant densities (30, 60, 90, or 120 plants per row) (Figure S3), and various morphological trait data were collected. Measurements were collected on plant height at three different time points during vegetative development and again at reproductive maturity (Table S2). *zmsut2-m1* mutant plants were consistently shorter than their wild-type siblings during vegetative growth, and this difference increased over time as the plants continued to develop (Table S2). However, at maturity (post-anthesis), in all planting densities, the mutants grew

Table 2. Photosynthesis-related traits from *zmsut2-m1* and wild-type (WT) leaves

Trait	Geno	*n*	Mean	Std Err	*P*-value
Vegetative					
Photos	WT	6	47.4	0.73	0.2561
	sut2-m1	6	45	1.93	
Cond	WT	6	0.35	0.04	0.3914
	sut2-m1	6	0.31	0.03	
SPAD	WT	6	59.8	1.8	0.0137*
	sut2-m1	6	53.6	1.08	
Maturity					
Photos	WT	6	44	1.5	0.355
	sut2-m1	6	46.6	2.3	
Cond	WT	6	0.35	0.03	0.9529
	sut2-m1	6	0.34	0.03	
SPAD	WT	6	61.5	1.35	0.1496
	sut2-m1	6	56.8	2.74	

Photos, photosynthesis (measured in μmol · m^{-2} s^{-1}); Cond, stomatal conductance (measured in mol · m^{-2} s^{-1}). SPAD is a relative unit of chlorophyll abundance. Geno, genotype; *n* = number of biological replicates; Std Err, standard error. *indicates traits that were significantly different at $P \leq 0.05$.

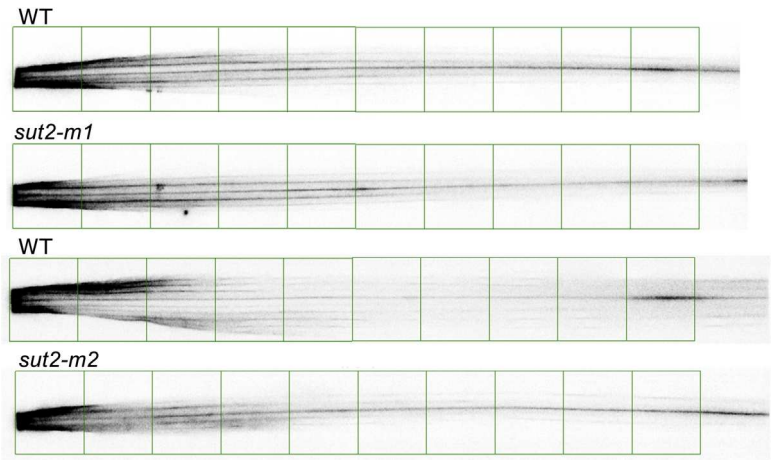

Figure 5. Autoradiographs depicting the transport of [^{18}F]-labeled sucrose in fully mature *zmsut2* mutant and wild-type (WT) source leaves
Green boxes represent 2.54 cm increments.

to >90% the height of wild type and were not significantly different at the 30 and 120 plants/row densities (Table S2). Further, contrary to our hypothesis, the growth deficiency of the *zmsut2-m1* mutants did not become more severe across planting densities at each time point. For example, at 60 days after planting, *zmsut2-m1* mutants displayed a 22%, 29%, 18%, and 26% reduction in height across the planting densities of 30, 60, 90, and 120 plants per row, respectively. In contrast, the tassel and ear lengths showed a progressive reduction with increasing plant density, with the *zmsut2-m1* mutants significantly smaller than wild type at all densities (Figure 6A; Table S2). The decrease in ear size also lead to a significant reduction in the total kernel number per ear, except at the lowest planting density (Figure 6B). Additionally, *zmsut2-m1* mutant kernels generally weighed less at the densities of 30 and 60 plants/row, with the latter displaying a significant reduction in kernel weight between mutant and wild type. However, kernel weights were not significantly different in the 30, 90, and 120 planting densities (Figure 6C). Stem node diameter, kernel row number, and tassel primary branch number were not different between the *zmsut2-m1* mutant and wild type for any of the planting densities (data not shown). Finally, at higher planting densities, *zmsut2-m1* mutant plants had significantly lower pseudo-yield values than wild-type sibling plants, indicating *ZmSut2* positively contributes to plant yield (Figure 6D).

DISCUSSION

A number of group 4 SUTs (e.g., OsSUT2, LjSUT4) have been shown to localize to the vacuolar membrane. Based on orthology to these group 4 SUTs and the presence of a predicted tonoplast targeting motif in the ZmSUT2 protein sequence (Reinders et al. 2012), we anticipated ZmSUT2 would localize to the tonoplast. As expected, a ZmSUT2-RFP fusion protein localized to the vacuolar membrane. The predicted topology and subcellular localization of the protein, as well as the H^+ gradient across the tonoplast, suggest ZmSUT2 is responsible for transporting sucrose across the tonoplast from the vacuolar lumen to the cytoplasm. We also observed accumulation of the ZmSUT2-RFP signal in other endomembrane system compartments, which is similar to results observed from transient expression of other group 4 SUT fluorescent protein fusions (Schneider et al. 2012). These authors suggested that this localization may be due to the fusion protein becoming trapped or mis-sorted as a result of the fluorescent tag.

ZmSut2 mRNA is broadly expressed and displays a diurnal expression pattern

In barley, Weschke et al. (2000) found *HvSut2* to be highly expressed in leaves and moderately expressed in roots and seeds. *OsSut2* was similarly expressed in multiple tissues, including leaves, stem, roots, and flowers (Eom et al. 2011). We found *ZmSut2* to be

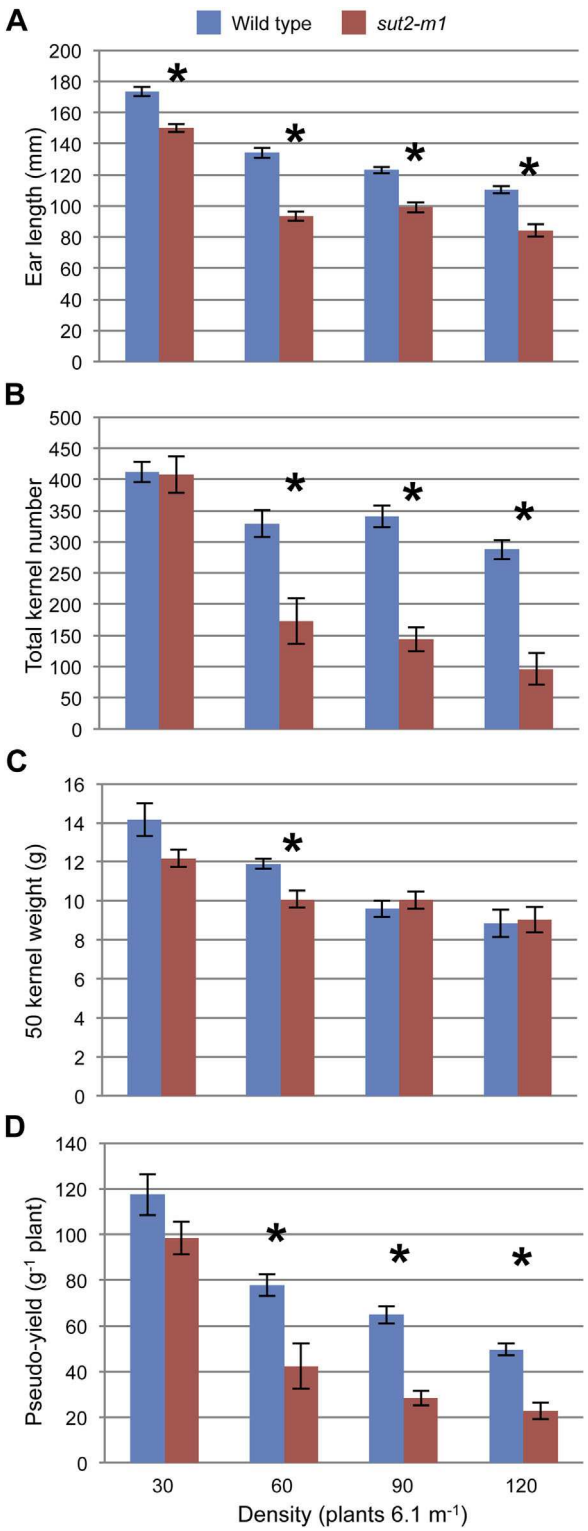

Figure 6. Histograms comparing *zmsut2-m1* mutants to wild-type sibling plants for (A) ear length, (B) total kernel number, (C) 50 kernel weight, and (D) pseudo-yield (measured in kernel g weight plant^{-1}) under four different planting densities grown in the field

Error bars represent standard error. An * indicates traits that were significantly different at $P \leq 0.05$.

moderately expressed in all tissues examined. In addition, broad expression has also been observed for related group 4 *Sut* genes in poplar (Payyavula et al. 2011), *Arabidopsis* (Weise et al. 2000; Schneider et al. 2012), and potato (Chincinska et al. 2008). Our analyses of *ZmSut2* mRNA levels supports the previous findings that group 4 *Suts* are ubiquitously expressed.

Interestingly, there are differences among species as to which tissue exhibits maximal gene expression for the group 4 *Suts*. The poplar, rice, and barley group 4 *Sut* genes displayed a similar expression pattern to *ZmSut2*, with greater expression occurring in source leaves as compared to sink leaves (Weschke et al. 2000; Eom et al. 2011; Payyavula et al. 2011). In contrast, in *Arabidopsis*, potato, and tomato, the group 4 *Suts* tend to be more highly expressed in sink leaves as compared to source leaves (Weise et al. 2000; Chincinska et al. 2008). An inference from these types of expression comparisons is that the various group 4 *Suts* may have different roles in different plants. However, this difference in expression may also be due to the time of day the tissue was harvested, since we observed significant variation in *ZmSut2* expression across diurnal time. Hence, care should be taken when comparing RNA abundance across different tissues without prior knowledge of the underlying diurnal expression pattern.

StSut4 mRNA displays a diurnal expression pattern in mature leaves, with peak expression occurring late in the afternoon (Chincinska et al. 2008). Similarly, we observed a peak in *ZmSut2* mRNA transcript levels between 4:30 pm and 8:30 pm. This diurnal cycling of the *ZmSut2* transcript also occurred in the immature sink leaves. Intriguingly, we found that expression in the immature sink leaf exceeded that of the mature source leaf for a period of time each day. Specifically, *ZmSut2* showed greater mRNA expression in mature adult leaves from midmorning to shortly after midnight when compared to the immature leaf. However, for about nine hours during the early morning, corresponding to the minima of *ZmSut2* RNA expression in source tissue, the expression was higher in the immature leaf. Additionally, the magnitude of the expression pattern for *ZmSut2* mRNA in the mature leaf displays a greater range with an approximately 22-fold expression change over a 24 h period, whereas expression in the immature leaf is more stable with only about a two-fold variation. One possible explanation is that the high *ZmSut2* expression in source leaves late in the day reflects the

cell preparing to efflux sucrose from the vacuole during the night. Conversely, during the early morning hours, when less sucrose is available for export from the vacuole, the reduced *ZmSut2* expression in source leaves could be important for allowing the cell to store the sucrose synthesized in the subsequent period of maximal photoassimilate accumulation. However, it is important to note that RNA expression levels and protein abundance are often not well correlated (Fernie and Stitt 2012). Future work is needed to examine ZmSUT2 protein levels over a diurnal cycle to determine whether the protein likewise cycles in abundance.

NSC accumulate in source leaves when group 4 *Sut* genes are knocked out

The localization and putative function of group 4 SUTs in sucrose efflux suggests a disruption in function would result in increased sugar levels in source leaves. Further, differences in sugar levels between group 4 *sut* mutant and wild-type leaves would be expected to be exacerbated in the early morning hours, since wild-type source leaves would have depleted their sucrose stores during the night to meet the demands of respiration, metabolism, and export. Based on this prediction, we sampled source leaves in the early morning hours and found that plants homozygous for either *zmsut2* mutant allele had significantly more sucrose and glucose compared to wild type. The amount of fructose was also greater in both mutants but only significantly different than wild type for the *zmsut2-m1* allele. Starch levels at the end of the night in both *zmsut2* mutant and wild-type leaves were low and relatively similar. Interestingly, the levels of sucrose and glucose, but not fructose, in rice *ossut2* mutant leaves at the end of the night were significantly greater compared to wild type (Eom et al. 2011), similar to our observations for *zmsut2* mutants. Likewise, in poplar, at the end of the night, sucrose was approximately 33% higher in mature leaves of *PtaSut4*-RNAi lines, but there was little difference between the two genotypes with regard to glucose and fructose levels (Payyavula et al. 2011). In contrast, there were no differences in sucrose, glucose, or fructose levels in *StSut4*-RNAi source leaves at the beginning of the day compared to wild type (Chincinska et al. 2008). Overall, with the exception of potato, these data show that sucrose, and sometimes glucose and fructose, is higher in the leaves of plants with reduced function in the group 4 *Sut* gene near dawn.

Similar to the two-fold increase in sugars observed in the source leaves of *ossut2* at the end of day (Eom et al. 2011), we also observed a two-fold increase in sucrose, glucose, fructose, and starch levels in source leaves of *zmsut2* mutant plants compared to wild type. In poplar leaves at the end of the day, sucrose was likewise approximately 1.5-fold higher in *PtaSut4*-RNAi lines, but little difference was observed between genotypes in terms of glucose and fructose levels (Payyavula et al. 2011). In *StSut4*-RNAi lines at the end of the day, glucose was consistently increased in all five independent transgenic lines analyzed, whereas fructose was increased in two out of five, and sucrose increased in three out of five (Chincinska et al. 2008). *atsut4* loss-of-function mutant seedlings do not accumulate excess sugars (Schneider et al. 2012). Hence, with the exception of *Arabidopsis*, mutations in group 4 *Sut* genes result in an approximate two-fold increase in sucrose in source leaves at the end of the day, with varying effects on glucose and fructose amounts.

In plants missing the group 4 *Sut* gene, one conserved mechanism for the remobilization of vacuolar sucrose could be the breakdown of some of the sucrose into glucose and fructose by vacuolar invertases, and the subsequent transport of these hexoses across the tonoplast by other families of sugar transporter proteins (Ruan et al. 2010; Martinoia et al. 2012). Once exported to the cytoplasm, the hexose sugars could be re-synthesized into sucrose, which would be available for long-distance transport. However, this synthetic route requires the energetic step of glucose phosphorylation (Sheen 2014). We hypothesize that the added energetic expense of the ATP needed to re-synthesize sucrose, coupled with the reduced availability of vacuolar-supplied sucrose for long-distance transport, results in the observed *zmsut2* and other group 4 *Sut* mutant phenotypes. Further research is needed to validate this hypothesis by examining the enzyme activities of vacuolar invertases, hexokinase, sucrose phosphate synthases, and sucrose synthases, as well as identifying the tonoplast-localized hexose transporters responsible for transporting glucose and fructose from the vacuolar lumen.

Finally, in comparing starch abundance in source leaves between dawn and dusk, it appears that the *zmsut2* mutants accumulate more starch than wild-type siblings at the end of the day, but metabolize their starch reserves completely to the same low level as wild-type

siblings by the end of the night to compensate for the reduced ability to mobilize sucrose out of the vacuole. Additionally, in sink leaves, *zmsut2* mutant plants contained significantly decreased amounts of glucose and starch, a slight, but not statistically significant increase in sucrose, and no difference with regards to fructose compared to wild type. The similar sucrose levels in immature *zmsut2* mutant and wild-type leaves suggests that long-distance sucrose transport or accumulation is not impaired in *zmsut2* plants (see below).

Role of group 4 SUTs in long-distance sucrose transport

Studies in other plant species suggest group 4 SUTs might contribute to sucrose transport in a source leaf. Chincinska et al. (2008) quantified sucrose efflux from petioles of excised leaves of *StSut4*-RNAi plants and found that sucrose export increased throughout the day, correlating with increased sucrose content in tubers and the shoot apical meristem, and an early transition to flowering. These results together with yeast two-hybrid studies, demonstrating that the orthologous SlSUT4 protein is able to interact with SlSUT1 (Reinders et al. 2002), led the researchers to hypothesize StSUT4 post-transcriptionally inhibits the function of StSUT1, the primary phloem loader in potato (Bürkle et al. 1998; Chincinska et al. 2008). In the *StSut4*-RNAi plants, this inhibition of *StSut1* function is hypothesized to be relieved, resulting in an increase in sucrose export. However, rice plants lacking *OsSut2* function exhibited decreased sugar export from a source leaf, which was interpreted as support for rice potentially using a modified form of symplasmic phloem loading (Eom et al. 2012), but see Braun et al. (2014) for discussion.

To evaluate whether the orthologous *ZmSut2* gene might functionally contribute to sucrose transport in a leaf, we used [^{18}F]-radiolabeled sucrose to examine sucrose movement in *zmsut2* mutant plants. We found no differences in the transport of sucrose from the apoplasmic space through the phloem between *zmsut2* mutants and their wild-type siblings. Hence, in contrast to the proposed role for a group 4 SUT in mediating symplasmic sucrose phloem loading in rice leaves (Eom et al. 2012), we found no evidence that ZmSUT2 directly contributes to long-distance sucrose movement in source leaves. However, given that both OsSUT2 and ZmSUT2 localize to the tonoplast, and the highly similar mutant phenotypes of *ossut2* and *zmsut2* plants, we hypothesize that both proteins perform the same function, namely, the intracellular transport of sucrose from the vacuole to the cytoplasm in photosynthetic cells. Subsequently, sucrose moves symplasmically cell-to-cell through PD from the photosynthetic cells toward the phloem. In the small veins of both maize and rice source leaves, where sucrose enters the phloem, the phloem CC/SE complex is virtually symplasmically isolated from surrounding cells, necessitating apoplasmic sucrose transport (Braun et al. 2014). Thus, it is interesting to consider that the loss of the group 4 *Sut* gene in maize and rice produces a remarkably similar mutant phenotype. This result is most likely explained by a comparable reduction in sucrose in the cytoplasm of photosynthetic cells in both mutant leaves. Hence, less sucrose would leave the photosynthetic cells and be available for apoplasmic efflux and uptake into the phloem to be transported long-distance to growing tissues. Therefore, reinterpreting the data of Eom et al. (2011), while not conclusive, may suggest that rice uses a similar phloem loading strategy as maize and the other characterized grasses (Evert et al. 1978; Thompson and Dale 1981; Robinson-Beers and Evert 1991; Evert et al. 1996; Bihmidine et al. 2015). Additional research is necessary to clarify the pathway by which rice loads sucrose into the phloem.

Group 4 *Sut* genes function in plant growth and development

To assess the contribution of *ZmSut2* to plant growth and development, we performed phenotypic analysis of the *zmsut2* mutant plants as compared to wild-type siblings. We found that plants homozygous for both mutant alleles showed a significant, similar decrease in plant growth. Eom et al. (2011) characterized a T-DNA insertion into *OsSut2* and observed a similar reduction in plant height in rice. Chincinska et al. (2008) also observed a reduction in internode elongation and leaf number in *StSut4*-RNAi potato plants. Collectively, these data indicate that group 4 SUTs are important for plant growth and development. However, an exception to this conclusion was seen in *Arabidopsis*. In congruence with the lack of excess sugar accumulation in leaves described above, *atsut4* mutants do not display any visible phenotype when grown under normal growth conditions, cold stress, or supplementation with 3% sucrose (Schneider et al. 2012). This suggests *Arabidopsis* may utilize other proteins to remobilize sugar stored in the

vacuole, for example, a tonoplast-localized SWEET protein (Chardon et al. 2013; Klemens et al. 2013).

Under our standard planting conditions in the field, which are designed for genetic studies and not agricultural production, impaired *ZmSut2* function modestly effects plant growth and development. Hence, we wanted to determine whether loss of *ZmSut2* function would have a significant consequence in a more typical agricultural setting. We chose to characterize *zmsut2-m1* under increasing plant–plant competition, since increasing planting density is the largest contributor to increasing maize yields over the last 50 years (Duvick 2005). Across planting densities, as observed in the initial plant height measurements, *zmsut2* mutant plants were always significantly smaller than their wild-type siblings throughout development. Interestingly, at maturity, *zmsut2* mutant plants attained approximately 90% of the wild-type plant height, with the 60 kernel planting density having the greatest negative impact on mutant growth. In the 30 kernel and 120 kernel planting densities, *zmsut2* mutant plant height was nearly identical to that of the wild-type plants. These data suggest that during vegetative growth, *zmsut2* mutant plants grow at a slower rate, but will eventually grow nearly as well as wild-type plants.

However, we observed dramatic decreases in the overall yield of *zmsut2* mutant plants compared with wild type as planting densities increased. These decreases were mostly due to a decrease in ear length as individual kernel size was not greatly impacted, except for a significant decrease in kernel weight in the 60 kernel planting density. Along with a reduction in the size of the maternal reproductive organ, the tassel was also significantly smaller than the wild type in each planting density. These patterns likely reflect that under increasing stress due to plant-plant competition, the plant sacrifices paternal reproductive productivity to maximize the probability of setting seed through the female.

To date, much of the research examining characteristics that lead to improved plant productivity under increasing plant-plant competition have focused on morphological traits, such as leaf angle, ear height, and plant height (Duvick 1977; Duvick 1992; Duvick et al. 2010). Here, we suggest a molecular mechanism for which improvement under increasing planting density might be selected. Experiments utilizing quantitative genetic tools, such as association genetics, to determine if selection at the *ZmSut2* locus has occurred to improve yield may help identify beneficial alleles, which can then be used for further crop improvement (Yu and Buckler 2006; Peiffer et al. 2014; Benson et al. 2015).

In summary, we examined the expression, subcellular localization, and biological function of ZmSUT2. Our results demonstrate that ZmSUT2 is a tonoplast-localized SUT that is likely responsible for sucrose efflux from the vacuolar lumen to the cytosol, that enhances plant growth and development, and that contributes to plant yield under agronomic cultivation conditions. In contrast to the proposed role for *OsSut2*, we found that *ZmSut2* has no apparent role in sucrose movement through the phloem, consistent with the proposal that maize utilizes an apoplasmic route for sucrose phloem loading. Given that there are reported differences in the pathways for sugar movement between maize and rice, it will be interesting to determine if overexpression of *ZmSut2* may lead to improvements in yield under increasing planting densities, although overexpression of the *OsSut2* cDNA under the control of the strong maize *Ubiquitin* promoter did not (Eom et al. 2011).

METHODS AND MATERIALS

Plant growth conditions

Maize (*Zea mays* L.) plants were grown in a greenhouse supplemented with 600 watt high-pressure sodium lighting (1,000 $\mu mol \cdot m^{-2} \cdot s^{-1}$ under a 16/8 h, 29 °C/22 °C light: dark regime. Plants were grown in three gallon pots containing a peat-based potting mix (ProMix BX, Hummert International, St. Louis, MO, USA), iron sulfate (0.3% v/v, Dyna Green, Hummert International), and 12:12:12 N:P:K fertilizer (1.5% v/v, Dyna Max, Hummert International) and watered daily. For field studies, plants were grown at the University of Missouri South Farm Agricultural Research Center.

Genetic stocks and genotyping

Two individual lines possessing a *Mutator* (*Mu*) transposable element in *ZmSut2* (v3,GRMZM2G307561; v4, Zm00001d041192) were isolated from the Trait Utility System for Corn (TUSC, Pioneer Hi-Bred; (Bensen et al. 1995)). Maize plants carrying the mutant allele were outcrossed to the inbred line B73 containing the

Mu Killer locus to silence *Mu* activity (Slotkin et al. 2003; Slotkin et al. 2005), and then backcrossed into B73 for three more generations to produce BC_4 plants, which were used for analyses. Genomic DNA was extracted according to Leach et al. (2016). Plants carrying the *ZmSut2* wild-type and *zmsut2* mutant alleles were identified via PCR genotyping (Table S1). PCR conditions were 95 °C for 2 min, followed by 35 cycles of 95 °C for 30 s, annealing for 30 s, 72 °C for 1 min, with a final elongation step of 72 °C for 5 min. PCR amplification products were separated on a 2% agarose gel and visualized with SybrSafe (Life Technologies, Carlsbad, CA, USA).

Reverse transcription PCR (RT-PCR) experiments

For the RT-PCR experiments, greenhouse-grown B73 plants were used. Tissue was harvested from five biological replicates of juvenile leaf 3 at the V3 stage, and roots, mature adult leaf 8, immature leaf 13, stem, and developing tassel of plants at the V8 stage. RNA isolation and cDNA synthesis were completed as described (Slewinski et al. 2008; Bihmidine et al. 2015). Fifty nanograms of cDNA was used for each RT-PCR.

Quantitative real-time PCR (qRT-PCR) time course experiments

qRT-PCR experiments examining *ZmSut2* expression over a diurnal cycle were conducted as described (Baker et al. 2016). Ten biological replicates were collected from 6-week-old B73 field-grown plants every 4 h over a 48 h interval.

ZmSUT2 protein localization

The coding sequence for the ZmSUT2 protein (Zm00001d041192_T003) followed by a linker of 10 alanine residues was synthesized in the pDONOR–221 vector (Life Technologies). The ZmSUT2 coding sequence was recombined into the pEarleyGate101 vector in which the mCherry (Red Fluorescent Protein, RFP) coding sequence replaced the yellow fluorescent protein tag (Ma et al. 2009) to generate the ZmSUT2-RFP translational fusion protein clone.

Maize mesophyll cell protoplasts were isolated according to Sheen (2001) from 10 d old etiolated leaves from B73. Thirty to 40 μg of the ZmSUT2-RFP plasmid DNA was added to approximately 3×10^5 protoplasts. Protoplasts were electroporated using a BTX ECM 600 with the following settings: capacitance of 200 μF, 240 V, and a resistance of 72 ohms, resulting in a time constant of ~11 msec. Electroporated protoplasts were incubated at room temperature for 22 h in the dark prior to examination by confocal microscopy. Bright-field and RFP fluorescence images, respectively, were taken using identical microscope and camera settings as described in Baker et al. (2016). The plasma membrane of protoplasts was gently lysed using Ficoll to release intact vacuoles according to Schneider et al. (2012) using 0.6 M mannitol in place of sorbitol.

Phenotypic analysis

Families segregating 1 (mutant): 1 (heterozygote) for either the *zmsut2-m1* or *zmsut2-m2* and wild-type alleles were planted in the field in 6.1 m rows, with 0.5 m width spacing between rows, at a density of 30 kernels per row. Plant height was determined by measuring the distance from soil level to the ligule of the topmost fully expanded leaf at 49 d after planting. Heights were measured across two replications. Since no statistical difference was found between the two replications, the data presented is the combination of the two, where the total numbers of individuals measured were 40 wild type (WT) and 40 *zmsut2-m1* mutants, and 43 WT and 22 *zmsut2-m2* mutants.

For the increased planting density experiments, seeds segregating 1:1 for the *zmsut2-m1* mutant and wild type were planted at increasing planting densities in 6.1 m rows that were 0.5 m apart. Densities were planted at 30 kernels, 60 kernels, 90 kernels, or 120 kernels per 6.1 m row (Figure S3). The first and last 1.5 m of each row, and the row adjacent to either side of the specified density block, were planted with B73 at the same planting density to shield the experimental plants from border effects. Trait data were collected for three replications. The data presented are for one replicate; however, significant differences and trends between WT and *zmsut2* mutants were similar among all three replications. Plant height measurements for the first replication were taken 33, 46, and 60 d after planting and at maturity (post-anthesis). Plant height measurements for the second and third replications were taken 23, 38, and 54 d after planting and at maturity. Open pollinated ears were collected at the end of the field season to measure ear length (30 kernel density $n = 23$ WT, 20 *zmsut2* mutants; 60 kernel density $n = 20$ WT, 22 *zmsut2*; 90 kernel density $n = 32$ WT, 32 *zmsut2*; 120 kernel density $n = 42$ WT, 14 *zmsut2*), kernel row

number, total seed set (30 kernel density $n = 12$ WT, 10 *zmsut2*; 60 kernel density $n = 11$ WT, 12 *zmsut2*; 90 kernel density $n = 12$ WT, 10 *zmsut2*; 120 kernel density $n = 10$ WT, 9 *zmsut2*), and 50 kernel weight set (30 kernel density $n = 12$ WT, 10 *zmsut2*; 60 kernel density $n = 11$ WT, 12 *zmsut2*; 90 kernel density $n = 12$ WT, 10 *zmsut2*; 120 kernel density $n = 10$ WT, 5 *zmsut2*). Pseudo-yield was calculated on a per plant basis by dividing the 50 kernel weight by 50 and multiplying by the total number of kernels present on the ear. Individuals in this study rarely produced a second ear and when a second ear was present it was barren. Tassels were also collected at maturity to measure length from the last node to the tip of the tassel and primary branch number. Leaf chlorophyll relative content was measured with a SPAD meter in the 30 kernel planting density 38 d after planting and at anthesis (Ma et al. 2008). The leaf measured at 38 d was the upper most fully expanded leaf. At anthesis, the leaf measured was either the first or second healthy leaf above the top ear node. At these developmental time points on the same individuals used for SPAD measurements, a LiCor 6400 was used to measure mid-morning (9:30 to 10:30 am) stomatal conductance and photosynthesis (Huang et al. 2009; Bihmidine et al. 2015).

Sugar and starch quantification

The non-structural carbohydrates (NSC) sucrose, glucose, fructose, and starch were extracted from 100 mg of fresh leaf tissue as described (Leach and Braun 2016). The neutral fraction of the extract was analyzed utilizing high performance anion exchange (HPAE) chromatography (ICS-5000, Thermo-Fisher Scientific). The HPAE was equipped with a SA10 column maintained at 45 °C. An isocratic 10 mmol/L potassium hydroxide solution was used as the eluent at a constant flow rate of 1.5 mL · min^{-1}. The manufacturer's recommended quadrupole wave form was used for detection with a disposable gold electrode maintained at 25 °C. Due to the sensitivity of the detector, samples were diluted 20- to 100-fold in water to ensure they fell within the linear range of the standard curve used to determine concentrations against known sugar standards. For mature leaf (lf 13) samples collected early in the morning, between 6:00 am and 7:30 am, two replications were quantified consisting of 4–6 individual plants per genotype per replicate. Upon analysis, no statistical significance was found between the two replications; hence, the data presented are the combination of both replications for which $n = 11$–12 individuals for both WT and the *zmsut2-m1* mutants, and $n = 8$–9 individuals for both WT and the *zmsut2-m2* mutants. Three replications of mature source leaves (lf 11) and immature sink leaves (lf 17) were collected at the end of day between 5:30 pm and 8:00 pm. Each biological replicate consisted of five to six individual leaf samples for both WT and *zmsut2-m1* mutants. The data presented are from one of those replications; however, significant differences and trends were similar among the replications.

[^{18}F]-labeled sucrose transport assay

Long-distance sucrose transport through a leaf was evaluated in greenhouse-grown *zmsut2* mutant and wild-type sibling plants according to Rotsch et al. (2015). Transport was measured on eight individuals each of both mutant and wild-type plants for both *zmsut2* mutant alleles.

Statistical analyses

Statistical significance was determined at the $P \leq 0.05$ level using the *Proc GLM* package in SAS (v 9.4).

ACKNOWLEDGEMENTS

We thank Dr. Frank Baker for instruction and assistance with confocal laser scanning microscopy and for providing critical feedback for improving the manuscript; Dr. Saadia Bihmidine for performing the photosynthesis and gas exchange measurements; and Michael Swyers, Jamie Hibbard, Erin Finefield, Brady Barron, Parker Brush, Tanner Buschmann, and Matt Boyer for assistance with phenotypic characterizations. We also thank Dr. Jim Birchler for use of the electroporator, Drs. Sherry Flint-Garcia and Tim Beissinger for helpful discussions, and Ben Julius and Dr. Rachel Mertz for comments that improved the manuscript. This research was supported by the National Science Foundation Plant Genome Research Program, grant no. IOS-1025976 to DMB.

AUTHOR CONTRIBUTIONS

K.A.L. participated in the design of the study, conducted the expression analysis, mutant molecular characterization, protein localization, sugar quantification, mutant

phenotypic characterization, statistical analyses and drafted the article; T.M.T. performed the radioactive sucrose transport assays; T.L.S. confirmed the *Mutator* insertions into the gene and performed genetic crosses; R.B.M. identified the *Mutator* insertions into the gene; D.M.B. conceived of the study, participated in its design and implementation, and helped draft the article; all authors edited and critically revised the article.

REFERENCES

Ainsworth EA, Bush DR (2011) Carbohydrate export from the leaf: A highly regulated process and target to enhance photosynthesis and productivity. **Plant Physiol** 155: 64–69

Aoki N, Hirose T, Scofield GN, Whitfeld PR, Furbank RT (2003) The sucrose transporter gene family in rice. **Plant Cell Physiol** 44: 223–232

Aoki N, Hirose T, Takahashi S, Ono K, Ishimaru K, Ohsugi R (1999) Molecular cloning and expression analysis of a gene for a sucrose transporter in maize (*Zea mays* L.). **Plant Cell Physiol** 40: 1072–1078

Ayre BG (2011) Membrane-transport systems for sucrose in relation to whole-plant carbon partitioning. **Mol Plant** 4: 377–394

Baker RF, Leach KA, Boyer NR, Swyers MJ, Benitez-Alfonso Y, Skopelitis T, Luo A, Sylvester A, Jackson D, Braun DM (2016) Sucrose transporter *ZmSut1* expression and localization uncover new insights into sucrose phloem loading. **Plant Physiol** 172: 1876–1898

Baker RF, Leach KA, Braun DM (2012) SWEET as sugar: New sucrose effluxers in plants. **Mol Plant** 5: 766–768

Bensen R, Johal G, Crane V, Tossberg J, Schnable P, Meeley R, Briggs S (1995) Cloning and characterization of the maize *An1* gene. **Plant Cell** 7: 75–84

Benson JM, Poland JA, Benson BM, Stromberg EL, Nelson RJ (2015) Resistance to gray leaf spot of maize: Genetic architecture and mechanisms elucidated through nested association mapping and near-isogenic line analysis. **PLoS Genet** 11: e1005045

Bihmidine S, Baker RF, Hoffner C, Braun DM (2015) Sucrose accumulation in sweet sorghum stems occurs by apoplasmic phloem unloading and does not involve differential *Sucrose transporter* expression. **BMC Plant Biol** 15: 186

Bihmidine S, Hunter III CT, Johns CE, Koch KE, Braun DM (2013) Regulation of assimilate import into sink organs: Update on molecular drivers of sink strength. **Front Plant Sci** 4: 177

Boorer KJ, Loo DDF, Frommer WB, Wright EM (1996) Transport mechanism of the cloned potato H^+/sucrose cotransporter StSUT1. **J Biol Chem** 271: 25139–25144

Braun DM (2012) SWEET! The pathway is complete. **Science** 335: 173–174

Braun DM, Slewinski TL (2009) Genetic control of carbon partitioning in grasses: Roles of *Sucrose Transporters* and *Tie-dyed* loci in phloem loading. **Plant Physiol** 149: 71–81

Braun DM, Wang L, Ruan YL (2014) Understanding and manipulating sucrose phloem loading, unloading, metabolism, and signalling to enhance crop yield and food security. **J Exp Bot** 65: 1713–1735

Bürkle L, Hibberd JM, Quick WP, Kühn C, Hirner B, Frommer WB (1998) The H^+-sucrose cotransporter NtSUT1 is essential for sugar export from tobacco leaves. **Plant Physiol** 118: 59–68

Carpaneto A, Geiger D, Bamberg E, Sauer N, Fromm J, Hedrich R (2005) Phloem-localized, proton-coupled sucrose carrier ZmSUT1 mediates sucrose efflux under the control of the sucrose gradient and the proton motive force. **J Biol Chem** 280: 21437–21443

Chandran D, Reinders A, Ward JM (2003) Substrate specificity of the *Arabidopsis thaliana* sucrose transporter AtSUC2. **J Biol Chem** 278: 44320–44325

Chardon F, Bedu M, Calenge F, Klemens PAW, Spinner L, Clement G, Chietera G, Léran S, Ferrand M, Lacombe B, Loudet O, Dinant S, Bellini C, Neuhaus HE, Daniel-Vedele F, Krapp A (2013) Leaf fructose content is controlled by the vacuolar transporter SWEET17 in *Arabidopsis*. **Curr Biol** 23: 697–702

Chen LQ, Qu XQ, Hou BH, Sosso D, Osorio S, Fernie AR, Frommer WB (2012) Sucrose efflux mediated by SWEET proteins as a key step for phloem transport. **Science** 335: 207–211

Chincinska IA, Liesche J, Krügel U, Michalska J, Geigenberger P, Grimm B, Kühn C (2008) Sucrose transporter StSUT4 from potato affects flowering, tuberization, and shade avoidance response. **Plant Physiol** 146: 515–528

Compaan B, Ruttink T, Albrecht C, Meeley R, Bisseling T, Franssen H (2003) Identification and characterization of a *Zea mays* line carrying a transposon-tagged ENOD40. **Biochim Biophys Acta** 1629: 84–91

Czedik-Eysenberg A, Arrivault S, Lohse MA, Feil R, Krohn N, Encke B, Nunes-Nesi A, Fernie AR, Lunn JE, Sulpice R, Stitt M (2016) The interplay between carbon availability and growth in different zones of the growing maize leaf. **Plant Physiol** 172: 943–967

Duvick D (1977) Genetic rates of gain in hybrid maize yields during the past 40 years. **Maydica** 22: 187–196

Duvick D (2005) Genetic progress in yield of United States maize (*Zea mays* L.). **Maydica** 50: 193–202

Duvick D, Smith J, Cooper M (2010) Long-term selection in a commercial hybrid maize breeding program. In Janick J, ed. *Plant Breeding Reviews. Part I*. John Wiley & Sons. pp. 109–152

Duvick DN (1992) Genetic contributions to advances in yield of US maize. **Maydica** 37: 69–79

Endler A, Meyer S, Schelbert S, Schneider T, Weschke W, Peters SW, Keller F, Baginsky S, Martinoia E, Schmidt UG (2006) Identification of a vacuolar sucrose transporter in

barley and *Arabidopsis* mesophyll cells by a tonoplast proteomic approach. **Plant Physiol** 141: 196–207

Eom JS, Chen LQ, Sosso D, Julius BT, Lin IW, Qu XQ, Braun DM, Frommer WB (2015) SWEETs, transporters for intracellular and intercellular sugar translocation. **Curr Opin Plant Biol** 25: 53–62

Eom J-S, Cho J-I, Reinders A, Lee S-W, Yoo Y, Tuan PQ, Choi S-B, Bang G, Park Y-I, Cho M-H, Bhoo SH, An G, Hahn T-R, Ward JM, Jeon J-S (2011) Impaired function of the tonoplast-localized sucrose transporter in rice, OsSUT2, limits the transport of vacuolar reserve sucrose and affects plant growth. **Plant Physiol** 157: 109–119

Eom J-S, Choi S-B, Ward JM, Jeon J-S (2012) The mechanism of phloem loading in rice (*Oryza sativa*). **Mol Cells** 33: 431–438

Evert RF, Eschrich W, Heyser W (1978) Leaf structure in relation to solute transport and phloem loading in *Zea mays* L. **Planta** 138: 279–294

Evert RF, Russin WA, Botha CEJ (1996) Distribution and frequency of plasmodesmata in relation to photoassimilate pathways and phloem loading in the barley leaf. **Planta** 198: 572–579

Fernie AR, Stitt M (2012) On the discordance of metabolomics with proteomics and transcriptomics: Coping with increasing complexity in logic, chemistry, and network interactions scientific correspondence. **Plant Physiol** 158: 1139–1145

Gil L, Yaron I, Shalitin D, Sauer N, Turgeon R, Wolf S (2011) Sucrose transporter plays a role in phloem loading in CMV-infected melon plants that are defined as symplastic loaders. **Plant J** 66: 366–374

Gottwald JR, Krysan PJ, Young JC, Evert RF, Sussman MR (2000) Genetic evidence for the *in planta* role of phloem-specific plasma membrane sucrose transporters. **Proc Natl Acad Sci USA** 97: 13979–13984

Hackel A, Schauer N, Carrari F, Fernie AR, Grimm B, Kühn C (2006) Sucrose transporter LeSUT1 and LeSUT2 inhibition affects tomato fruit development in different ways. **Plant J** 45: 180–192

Hirose T, Imaizumi N, Scofield GN, Furbank RT, Ohsugi R (1997) cDNA cloning and tissue specific expression of a gene for sucrose transporter from rice (*Oryza sativa* L.). **Plant Cell Physiol** 38: 1389–1396

Hirose T, Zhang Z, Miyao A, Hirochika H, Ohsugi R, Terao T (2010) Disruption of a gene for rice sucrose transporter, *OsSUT1*, impairs pollen function but pollen maturation is unaffected. **J Exp Bot** 61: 3639–3646

Huang M, Slewinski TL, Baker RF, Janick-Buckner D, Buckner B, Johal GS, Braun DM (2009) Camouflage patterning in maize leaves results from a defect in porphobilinogen deaminase. **Mol Plant** 2: 773–789

Ishimaru K, Hirose T, Aoki N, Takahashi S, Ono K, Yamamoto S, Wu J, Saji S, Baba T, Ugaki M, Matsumoto T, Ohsugi R (2001) Antisense expression of a rice sucrose transporter OsSUT1 in rice (*Oryza sativa* L.). **Plant Cell Physiol** 42: 1181–1185

Kaiser G, Heber U (1984) Sucrose transport into vacuoles isolated from barley mesophyll protoplasts. **Planta** 161: 562–568

Klemens PAW, Patzke K, Deitmer J, Spinner L, Le Hir R, Bellini C, Bedu M, Chardon F, Krapp A, Neuhaus HE (2013) Overexpression of the vacuolar sugar carrier *AtSWEET16* modifies germination, growth, and stress tolerance in *Arabidopsis*. **Plant Physiol** 163: 1338–1352

Ko DK, Rohozinski D, Song Q, Taylor SH, Juenger TE, Harmon FG, Chen ZJ (2016) Temporal shift of circadian-mediated gene expression and carbon fixation contributes to biomass heterosis in maize hybrids. **PLoS Genet** 12: e1006197

Kühn C, Grof CPL (2010) Sucrose transporters of higher plants. **Curr Opin Plant Biol** 13: 287–297

Lalonde S, Wipf D, Frommer WB (2004) Transport mechanisms for organic forms of carbon and nitrogen between source and sink. **Annu Rev Plant Biol** 55: 341–372

Leach KA, Braun DM (2016) Soluble sugar and starch extraction and quantification from maize leaves. **Curr Prot Plant Biol** 1: 139–161

Leach KA, McSteen PC, Braun DM (2016) Genomic DNA isolation from maize (*Zea mays*) leaves using a simple, high-throughput protocol. **Curr Prot Plant Biol** 1: 15–27

Lucas WJ, Groover A, Lichtenberger R, Furuta K, Yadav SR, Helariutta Y, He XQ, Fukuda H, Kang J, Brady SM, Patrick JW, Sperry J, Yoshida A, López-Millán AF, Grusak MA, Kachroo P (2013) The plant vascular system: Evolution, development and functions. **J Int Plant Biol** 55: 294–388

Lucas WJ, Lee JY (2004) Plasmodesmata as a supracellular control network in plants. **Nat Rev Mol Cell Biol** 5: 712–726

Ma Y, Baker RF, Magallanes-Lundback M, DellaPenna D, Braun DM (2008) *Tie-dyed1* and Sucrose export defective1 act independently to promote carbohydrate export from maize leaves. **Planta** 227: 527–538

Ma Y, Slewinski TL, Baker RF, Braun DM (2009) *Tie-dyed1* encodes a novel, phloem-expressed transmembrane protein that functions in carbohydrate partitioning. **Plant Physiol** 149: 181–194

Martinoia E, Meyer S, De Angeli A, Nagy R (2012) Vacuolar transporters in their physiological context. **Annu Rev Plant Biol** 63: 183–213

Okubo-Kurihara E, Higaki T, Kurihara Y, Kutsuna N, Yamaguchi J, Hasezawa S (2011) Sucrose transporter NtSUT4 from tobacco BY-2 involved in plant cell shape during mini-protoplast culture. **J Plant Res** 124: 395–403

Payyavula RS, Tay KH, Tsai CJ, Harding SA (2011) The sucrose transporter family in *Populus*: The importance of a tonoplast PtaSUT4 to biomass and carbon partitioning. **Plant J** 65: 757–770

Peiffer JA, Romay MC, Gore MA, Flint-Garcia SA, Zhang Z, Millard MJ, Gardner CA, McMullen MD, Holland JB, Bradbury PJ (2014) The genetic architecture of maize height. **Genetics** 196: 1337–1356

Peng D, Gu X, Xue LJ, Leebens-Mack JH, Tsai CJ (2014) Bayesian phylogeny of sucrose transporters: Ancient

origins, differential expansion and convergent evolution in monocots and dicots. **Frontiers in Plant Science** 5: 615

Raizada M, Benito M, Walbot V (2001) The *MuDR* transposon terminal inverted repeat contains a complex plant promoter directing distinct somatic and germinal programs. **Plant J** 25: 79–91

Reinders A, Schulze W, Kuhn C, Barker L, Schulz A, Ward JM, Frommer WB (2002) Protein-protein interactions between sucrose transporters of different affinities colocalized in the same enucleate sieve element. **Plant Cell** 14: 1567–1577

Reinders A, Sivitz A, Starker C, Gantt J, Ward JM (2008) Functional analysis of LjSUT4, a vacuolar sucrose transporter from *Lotus japonicus*. **Plant Mol Biol** 68: 289–299

Reinders A, Sivitz AB, Ward JM (2012) Evolution of plant sucrose uptake transporters. **Front Plant Sci** 3: 22

Rennie EA, Turgeon R (2009) A comprehensive picture of phloem loading strategies. **Proc Natl Acad Sci USA** 106: 14162–14167

Riesmeier JW, Willmitzer L, Frommer WB (1992) Isolation and characterization of a sucrose carrier cDNA from spinach by functional expression in yeast. **EMBO J** 11: 4705–4713

Riesmeier JW, Willmitzer L, Frommer WB (1994) Evidence for an essential role of the sucrose transporter in phloem loading and assimilate partitioning. **EMBO J** 13: 1–7

Robinson-Beers K, Evert RF (1991) Ultrastructure of and plasmodesmatal frequency in mature leaves of sugarcane. **Planta** 184: 291–306

Rolland F, Baena-Gonzalez E, Sheen J (2006) Sugar sensing and signaling in plants: Conserved and novel mechanisms. **Annu Rev Plant Biol** 57: 675–709

Rotsch D, Brossard T, Bihmidine S, Ying W, Gaddam V, Harmata M, Robertson JD, Swyers M, Jurisson SS, Braun DM (2015) Radiosynthesis of 6'-deoxy-6'[^{18}F]fluorosucrose via automated synthesis and its utility to study *in vivo* sucrose transport in maize (*Zea mays*) leaves. **PLoS ONE** 10: e0128989

Ruan YL (2014) Sucrose metabolism: Gateway to diverse carbon use and sugar signaling. **Annu Rev Plant Biol** 65: 33–67

Ruan YL, Jin Y, Yang YJ, Li GJ, Boyer JS (2010) Sugar input, metabolism, and signaling mediated by invertase: Roles in development, yield potential, and response to drought and heat. **Mol Plant** 3: 942–955

Sauer N (2007) Molecular physiology of higher plant sucrose transporters. **FEBS Lett** 581: 2309–2317

Schneider S, Hulpke S, Schulz A, Yaron I, Höll J, Imlau A, Schmitt B, Batz S, Wolf S, Hedrich R, Sauer N (2012) Vacuoles release sucrose via tonoplast-localised SUC4-type transporters. **Plant Biol** 14: 325–336

Scofield G, Hirose T, Gaudron J, Upadhyaya N, Ohsugi R, Furbank RT (2002) Antisense suppression of the rice sucrose transporter gene, *OsSUT1*, leads to impaired grain filling and germination but does not affect photosynthesis. **Funct Plant Biol** 29: 815–826

Sheen J (2001) Signal transduction in maize and *Arabidopsis* mesophyll protoplasts. **Plant Physiol** 127: 1466–1475

Sheen J (2014) Master regulators in plant glucose signaling networks. **J Plant Biol** 57: 67–79

Slewinski TL, Braun DM (2010a) Current perspectives on the regulation of whole-plant carbohydrate partitioning. **Plant Sci** 178: 341–349

Slewinski TL, Braun DM (2010b) The *psychedelic* genes of maize redundantly promote carbohydrate export from leaves. **Genetics** 185: 221–232

Slewinski TL, Garg A, Johal GS, Braun DM (2010) Maize SUT1 functions in phloem loading. **Plant Sig Behav** 5: 687–690

Slewinski TL, Ma Y, Baker RF, Huang M, Meeley R, Braun DM (2008) Determining the role of *Tie-dyed1* in starch metabolism: Epistasis analysis with a maize ADP-glucose pyrophosphorylase mutant lacking leaf starch. **J Hered** 99: 661–666

Slewinski TL, Meeley R, Braun DM (2009) *Sucrose transporter1* functions in phloem loading in maize leaves. **J Exp Bot** 60: 881–892

Slotkin RK, Freeling M, Lisch D (2003) *Mu Killer* causes the heritable inactivation of the *Mutator* family of transposable elements in *Zea mays*. **Genetics** 165: 781–797

Slotkin RK, Freeling M, Lisch D (2005) Heritable transposon silencing initiated by a naturally occurring transposon inverted duplication. **Nat Genet** 37: 641–644

Smith AM, Stitt M (2007) Coordination of carbon supply and plant growth. **Plant Cell Environ** 30: 1126–1149

Srivastava AC, Ganesan S, Ismail IO, Ayre BG (2008) Functional characterization of the *Arabidopsis thaliana* AtSUC2 Suc/H^+ symporter by tissue-specific complementation reveals an essential role in phloem loading but not in long-distance transport. **Plant Physiol** 147: 200–211

Stelpflug SC, Sekhon RS, Vaillancourt B, Hirsch CN, Buell CR, de Leon N, Kaeppler SM (2016) An expanded maize gene expression atlas based on RNA sequencing and its use to explore root development. **Plant Genome** 9: doi: 10.3835/plantgenome2015.3804.0025

Thompson R, Dale J (1981) Export of ^{14}C- and ^{11}C-labelled assimilate from wheat and maize leaves: Effects of parachloromercurobenzylsulphonic acid and fusicoccin and of potassium deficiency. **Can J Bot** 59: 2439–2444

Weise A, Barker L, Kühn C, Lalonde S, Buschmann H, Frommer WB, Ward JM (2000) A new subfamily of sucrose transporters, SUT4, with low affinity/high capacity localized in enucleate sieve elements of plants. **Plant Cell** 12: 1345–1355

Weschke W, Panitz R, Sauer N, Wang Q, Neubohn B, Weber H, Wobus U (2000) Sucrose transport into barley seeds: Molecular characterization of two transporters and implications for seed development and starch accumulation. **Plant J** 21: 455–467

Yadav UP, Ayre BG, Bush DR (2015) Transgenic approaches to altering carbon and nitrogen partitioning in whole plants: Assessing the potential to improve crop yields and nutritional quality. **Front Plant Sci** 6: 275

Yu J, Buckler ES (2006) Genetic association mapping and genome organization of maize. **Curr Opin Biotech** 17: 155–160

Zhang C, Han L, Slewinski TL, Sun J, Zhang J, Wang ZY, Turgeon R (2014) Symplastic phloem loading in poplar. **Plant Physiol** 166: 306–313

Zhang C, Turgeon R (2009) Downregulating the sucrose transporter *VpSUT1* in *Verbascum phoeniceum* does not inhibit phloem loading. **Proc Natl Acad Sci USA** 106: 18849–18854

SUPPORTING INFORMATION

Additional Supporting Information may be found online in the supporting information tab for this article: http://onlinelibrary.wiley.com/doi/10.1111/jipb.12527/suppinfo

Figure S1. Quantification of the amount of starch present in leaf 13 (in mg · g^{-1} FW) at the end of the night

Error bars represent standard error. Mutants were not statistically different from wild-type (WT) siblings.

Figure S2. Histograms of the amount of [^{18}F]-labeled sucrose present in 2.54 cm increments from the leaf tip (zero position) in (**A**) *zmsut2-m1* and wild-type plants, and in (**B**) *zmsut2-m2* and wild-type plants

Error bars represent standard error. No significant differences were observed between *zmsut2* mutant and wild type.

Figure S3. Images taken at the same distance from the plants to illustrate increasing planting density in a 6.1 m row of (**A**) 30 kernels, (**B**) 60 kernels, (**C**) 90 kernels, and (**D**) 120 kernels

Table S1. Primer sequences and PCR conditions for the primers utilized for genotyping, RT-PCR, and qRT-PCR

Table S2. Plant height and tassel length comparisons between *zmsut2-m1* and wild-type (WT) plants grown under increasing plant density

Plant height (cm) was measured at four time points throughout development as indicated by days after planting (DAP) or at maturity (post-anthesis). Tassel length was measured in cm after anthesis. N represents the number of biological replicates, std err represents the standard error, and an * indicates traits that were significantly different at $P \leq 0.05$.

Scan using WeChat with your smartphone to view JIPB online

Scan with iPhone or iPad to view JIPB online